

Paper-Based Electroanalytical Devices with an Integrated, Stable Reference Electrode

Wen-Jie Lan^a, E. Jane Maxwell^a, Claudio Parolo^{a,b}, David K. Bwambok^a, Anand Bala
Subramaniam^a, and George M. Whitesides^{a,c*}

^a Department of Chemistry and Chemical Biology, Harvard University, Cambridge, MA 02138

^b Nanobioelectronics & Biosensors Group, Institut Català de Nanotecnologia, CIN2, Campus
UAB, Barcelona, Spain

^c Wyss Institute for Biologically Inspired Engineering, Harvard University, Cambridge, MA
02138

*Corresponding author E-mail: gwhitesides@gmwgroup.harvard.edu

Supporting Information

Experimental

Chemicals: Carbon ink (E3456) and Ag/AgCl ink (E2414) were purchased from Ercon Inc. (Wareham, MA). Potassium nitrate (KNO_3) was purchased from Alfa Aesar. Potassium chloride (KCl), potassium ferricyanide ($\text{K}_3[\text{Fe}(\text{CN})_6]$), potassium hexachloroiridate (IV) (K_2IrCl_6), ferrocene ($\text{Fe}(\text{C}_5\text{H}_5)_2$), hexaammineruthenium (III) chloride ($\text{Ru}(\text{NH}_3)_6\text{Cl}_3$), tetrabutylammonium hexafluorophosphate (TBAPF_6), and acetonitrile were purchased from Sigma-Aldrich and used as received.

Electrochemical Supplies: Glassy carbon disk working electrodes (3-mm diameter, part # CHI 104) and Ag/AgCl reference electrodes with 1 M KCl internal filling solution (Part # CHI 111) were purchased from CH Instruments, Inc. A platinum gauze (Stock # 10283, Alfa Aesar) was used as the counter electrode. The working electrodes were polished before voltammetric experiments using a polishing kit (CHI 120) from CH Instruments.

Fabrication and Use of the Device: Paper-based zones and microfluidic channels were fabricated by patterning chromatography paper (Whatman 1 Chr) by wax printing. We fabricated electrochemical analytical devices by stencil-printing carbon ink or Ag/AgCl ink on the wax-printed paper. We generated a stencil for printing by designing patterns of electrodes using AutoCAD[®] 2012, and cut the pattern into frisket film (Grafix, low tack) using a laser-cutter (VersaLASER VLS3.50, Universal Laser Systems Inc.). We adhered the stencil on top of the paper, and filled the openings of the stencil with ink. We cured the ink by baking the electrodes in an oven at ~ 100 °C for 15-20 min. After the ink dried, we removed the film carefully. The reference and sample solutions were added to the corresponding zones using a pipette. For the

sealed devices, we cut and attached Fellowes[®] self-adhesive sheet (Staples) to the top and bottom of the device to minimize the effect of evaporation.

Device Geometry: The carbon working electrode is a 1.5-mm diameter disk electrode, while the carbon counter electrode has a larger surface area and surrounds the working electrode (Figure 1). For voltammetric applications, we designed rEPADs such that the carbon working and counter electrodes were stencil-printed on the right side of the device and the Ag/AgCl reference electrode (Ag/AgCl ink associated with the KCl solution) on the left side.

Cyclic Voltammetry: We performed cyclic voltammetry (CV) with paper-based devices (or a commercial electrochemical cell) and a potentiostat (Pine Instrument Co., AFCBP1) interfaced to a computer through a PCI-MIO-16E-4 data acquisition board (National Instruments) for potential and current measurements. Voltammetric data were recorded using in-house virtual instrumentation Pinechem 2.7.9a (Pine Instruments).

Convection in the Paper-Based Devices

Because we pipetted the same small amount of the solution (10 μL) to each zone, the mass transfer in the fluid-filled channel due to convection is negligible, *i.e.*, the convection is not strong enough to drive the solution from one side of the device to the other. In fact, even when 10 μL was applied only to the left zone, the solution stopped at the right-hand part of the microfluidic channel and did not wick into the right zone. Applications of convective flow in paper-based devices are detailed elsewhere (see reference 1).

Lifetime of Paper-Based Devices

We investigated the effect of sealing the devices with tape on the working time of the rEPADs without printed electrodes. Sealed devices require much longer times for the solutions to wick into the central mixing zone, compared to uncovered (Figure S1) devices (~15 min vs. ~0.5 min), because the air that initially occupies the central channel must diffuse through the tape or through the sides of the device as it is displaced by the sample and reference solutions. The uncovered devices dried completely within 20 minutes, while the sealed devices remained wet for more than 12 h. The color of the paper with CoCl_2 solution changed from pink to blue after the water had evaporated. In Figure 2f, the yellow color in the central contact zone might be due to the precipitation of various crystals including CuCl_2 , CoSO_4 , CoCl_2 , and CuSO_4 .

The lifetime for the rEPADs with printed electrodes is significantly shorter than the drying time for the unprinted devices because the electrodes creates a gap between the paper layer and the tape layer that allows water vapor to escape. This gap, however, can be filled by inserting a layer of parafilm or other filler materials, if longer device lifetime is desired.

Cost of Voltammetric rEPADs

We estimate the cost of materials of rEPADs to be ~\$0.06 per device. Ag/AgCl ink costs \$1 per gram, and one gram of ink is sufficient to produce thirty devices by manual stencil printing (\$0.033 per device). Graphite ink costs \$0.20 per gram, and one gram of graphite ink produces twenty devices by manual stencil printing (\$0.01 per device). One page of wax-printed paper (20 cm by 20 cm, 28 devices) costs ~\$0.50 (\$0.018 per device). Thus, one device costs \$0.061 in total. We estimate the cost of one device could be as low as \$0.04 using a mixed

Ag/AgCl/graphite ink as the reference electrode material. The estimation above is based on the price of commercial products.

Quantitative Measurements by Cyclic Voltammetry

The stability of the voltage measurement provided by the rEPAD allows us to use cyclic voltammetry to obtain quantitative information about the concentration of analyte. Figure S3a demonstrates a linear relationship between the peak current, i_p , at 0.19 V (vs. Ag/AgCl) and the concentration of $K_3[Fe(CN)_6]$ in the range of 1 to 10 mM (a typical range for cyclic voltammetry), in agreement with the Randles-Sevcik equation (eq S1).

$$i_p = (2.69 \times 10^5) n^{3/2} A D_o^{1/2} C_o^* \nu^{1/2} \quad (S1)$$

In this equation, n is the number of electrons transferred per analyte, A is the electrode area, D_o is the diffusion coefficient of the analyte, C_o^* is the bulk concentration of the analyte, and ν is the scan rate of the applied potential (V/s).

Cyclic voltammetry is not an ideal method for accurate quantitation of electroactive species, because the correction for the non-Faradaic charging current is typically uncertain. When properly referenced, the method does, however, provide an estimate of the analyte concentration; more importantly, the peak potentials, and the shape of the voltammetric curves, provide a qualitative study of redox processes and an understanding of the electrochemical mechanism of the system.

Figure S3b shows that the cathodic peak current is linearly proportional to the square root of the scan rate ($\nu^{1/2}$) in the rEPAD; this result indicates a reversible wave and diffusion-controlled mass transfer towards the working electrode, in accordance with the expected characteristics of the ferri/ferrocyanide redox couple.

rEPADs for multiplexed voltammetry

The potential differences between the anodic and cathodic peak potentials (ΔE_p) of $\text{Ru}(\text{NH}_3)_6^{3+/2+}$ and $\text{IrCl}_6^{2-/3-}$ were 88.4 and 86.4 mV, respectively (Figure 4). These values are slightly higher than the theoretical value for an ideal reversible one-electron redox system (59 mV at 25 °C), and may result from the ohmic resistance of the solution.²

Acetonitrile was used to dissolve the ferrocene and tetrabutyl ammonium hexafluorophosphate (TBAPF₆). The wax boundaries contained the acetonitrile within the hydrophilic region as long as only a small volume of solution (several μL) was used. Other cross-linked polymers that define channels—*e.g.*, SU-8³—would resist dissolution for longer, but were not required here. The applicability of this system is currently limited by evaporation, and the long-term incompatibility of electrochemical organic solvents with the wax barrier and the adhesive tape, but could be improved with further engineering and careful choice of materials.

We speculate that the relatively large capacitive current for the ferrocene/ferrocenium redox couple in acetonitrile (Figure 4c) is due to the interaction between the rough surface of the carbon electrode and the organic solvents used in the paper-based device. The peak splitting (~ 0.2 V) is often observed as a consequence of the sluggish, heterogeneous kinetics at the surface of the carbon electrodes.⁴ Quantitative analysis of samples in organic solvents by rEPADs may be affected by the relatively high instability of the interface between the organic solvent and the aqueous reference solution. The signal/noise ratio, however, can be increased upon reducing the scan rate of the voltage.⁵

Table S1 Applications of paper-based electroanalytical devices

Reference	Species detected/quantified	Electrochemical method
Nie et al. [6,7]	Glucose, lactate, ethanol, and heavy-metal ions	Chronoamperometry, cyclic voltammetry, anodic stripping voltammetry
Carvalho et al. [8]	ascorbic acid and uric acid	Amperometry
Henry et al. [9]	Glucose, lactate, uric acid, Au, and iron	Chronoamperometry, cyclic voltammetry, square wave voltammetry
Yu et al. [10]	Immunosensor (carcinoembryonic antigen (CEA) et al.)	Differential pulse voltammetry
Lankelma et al. [1]	Glucose	Amperometry
Liu et al. [11]	Adenosine, glucose, H ₂ O ₂	Amperometry, cyclic voltammetry
Shiroma et al. [12]	paracetamol, 4-aminophenol	Amperometry
Knoll et al. [13]	K ⁺ , Na ⁺	Potentiometry
Novell et al. [14]	NH ₄ ⁺ , K ⁺ , pH	Potentiometry

Figure S1. Photographs of a paper-based microfluidic device taken after adding distilled water and pink solution of CoCl_2 to corresponding zones. The CoCl_2 solution mixed with the water in the central zone but did not diffuse into the left paper zone. The color of the CoCl_2 solution became paler after 5 min and blue after 10 min as the device gradually dried out because of solvent evaporation. The device was not sealed with tape.

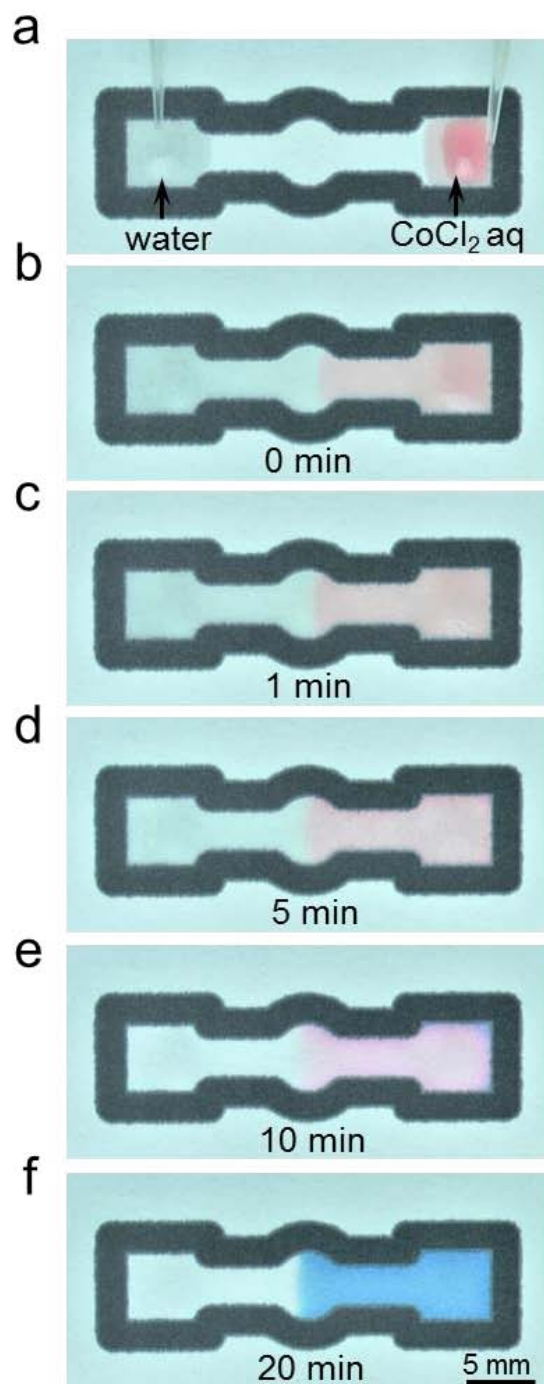


Figure S2. (a) Photograph and schematic illustration of a commercial Ag/AgCl reference electrode. (b) Front view and back view of a paper-based electrochemical device (rEPAD). The paper was patterned by wax printing to define the sample zone, central mixing zone, reference zone, and microfluidic channels. The sample and reference zones include stencil-printed carbon and Ag/AgCl electrodes, respectively. The arrows with the same number as in (a) refer to similar functions. The dashed lines indicate the approximate boundaries of the carbon and Ag/AgCl ink printed on the back.

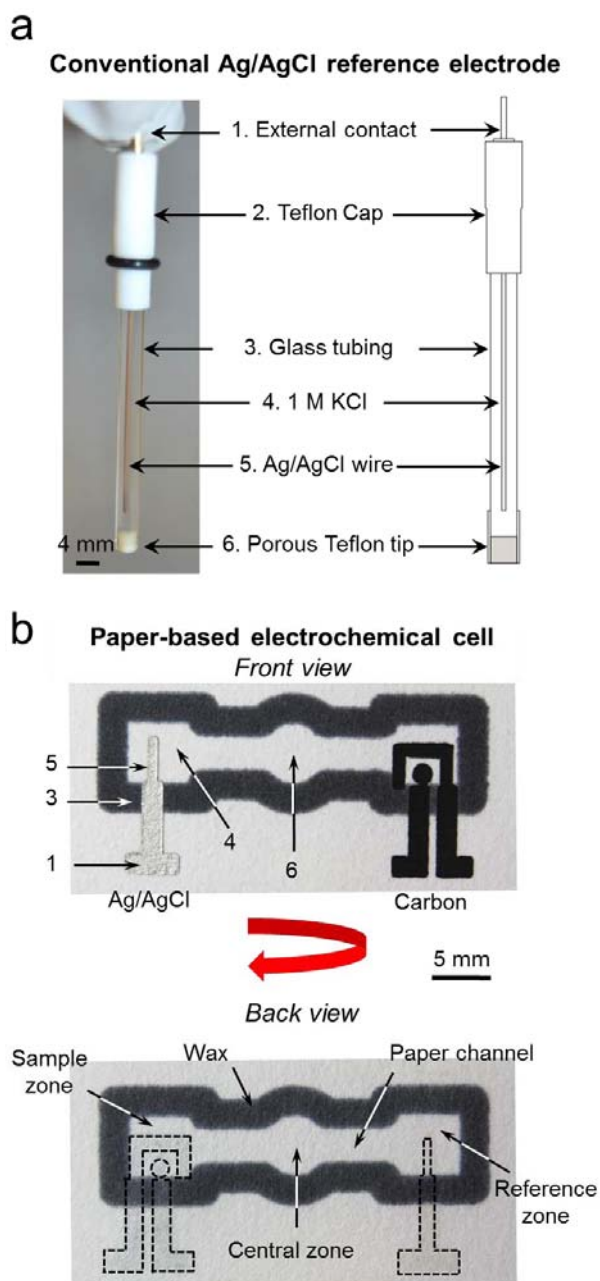
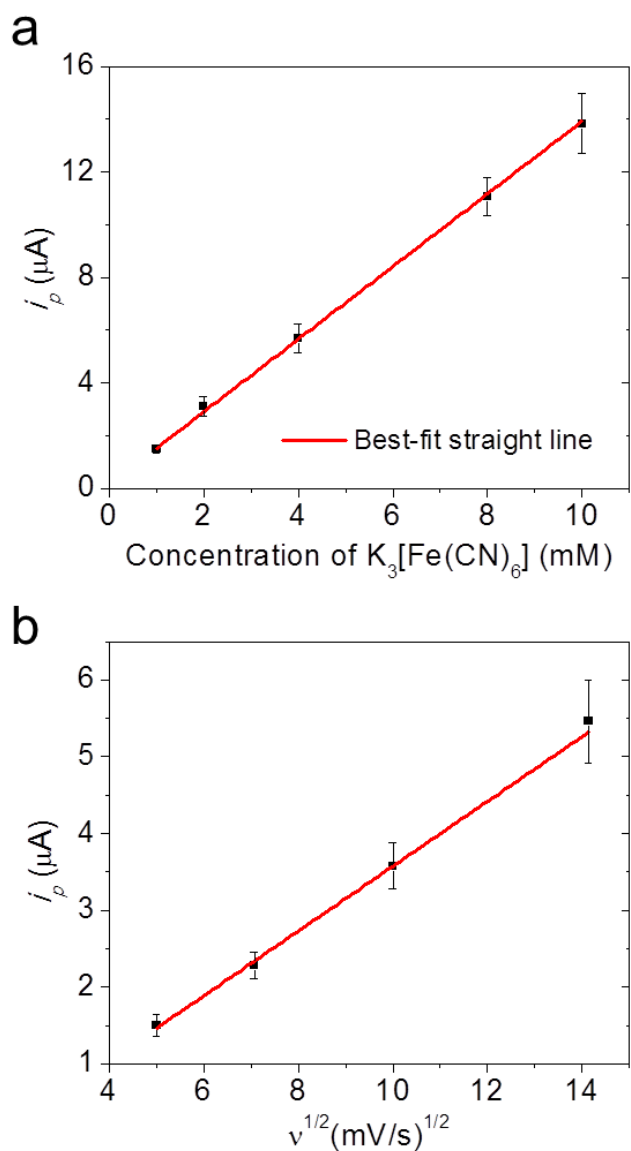


Figure S3. Cathodic peak current (i_p) as a function of (a) the concentration of $K_3[Fe(CN)_6]$ and (b) the square root of the scan rate ($v^{1/2}$) for cyclic voltammetry experiments conducted on rEPADs. The solid lines represent a linear fit to (a) with regression equation: $y = 0.16 + 1.4x$ ($R^2 = 0.998$, $n = 7$), and a linear fit to (b) in e with regression equation: $y = -0.65 + 0.42x$ ($R^2 = 0.995$, $n = 7$).



References

1. Lankelma, J.; Nie, Z.; Carrilho, E.; Whitesides, G. M. *Anal. Chem.* **2012**, *84*, 4147-4152.
2. Flanagan, J. B.; Margel, S.; Bard, A. J.; Anson, F. C. *J. Am. Chem. Soc.* **1978**, *100*, 4248-4253.
3. SU-8 2000.5-2015 Data Sheet, MicroChem Corp. (<http://www.microchem.com/Prod-SU82000.htm>)
4. Wang, J.; Pedrero, M.; Sakslund, H.; Hammerich, O.; Pingarron, J. *Analyst* **1996**, *121*, 345-350.
5. Bard, A. J.; Faulkner, L. R. *Electrochemical Methods: Fundamentals and Applications*, 2nd ed.; John Wiley & Sons: New York, 2001.
6. Nie, Z. H.; Nijhuis, C. A.; Gong, J. L.; Chen, X.; Kumachev, A.; Martinez, A. W.; Narovlyansky, M.; Whitesides, G. M. *Lab Chip* **2010**, *10*, 477-483.
7. Nie, Z. H.; Deiss, F.; Liu, X. Y.; Akbulut, O.; Whitesides, G. M. *Lab Chip* **2010**, *10*, 3163-3169.
8. Carvalho, R. F.; Kfoury, M. S.; de Oliveira Piazzetta, M. H.; Gobbi, A. L.; Kubota, L. T. *Anal. Chem.* **2010**, *82*, 1162-1165.
9. (a) Dungchai, W.; Chailapakul, O.; Henry, C. S. *Anal. Chem.* **2009**, *81*, 5821-5826. (b) Dungchai, W.; Chailapakul, O.; Henry, C. S. *Analyst* **2011**, *136*, 77-82. (c) Apilux, A.; Dungchai, W.; Siangproh, W.; Praphairaskit, N.; Henry, C. S.; Chailapakul, O. *Anal. Chem.* **2010**, *82*, 1727-1732.
10. (a) Zang, D.; Ge, L.; Yan, M.; Song, X.; Yu, J. *Chem. Commun.* **2012**, *48*, 4683-4685. (b) Wang, P.; Ge, L.; Yan, M.; Song, X.; Ge, S.; Yu, J. *Biosens. Bioelectron.* **2012**, *32*, 238-243.
11. (a) Liu, H.; Xiang, Y.; Lu, Y.; Crooks, R. M. *Angew. Chem. Int. Ed.* **2012**, *51*, 6925-6928. (b) Liu, H.; Crooks, R. M. *Anal. Chem.* **2012**, *84*, 2528-2532.
12. Shiroma, L. Y.; Santhiago, M.; Gobbi, A. L.; Kubota, L. T. *Anal. Chim. Acta* **2012**, *725*, 44-50.
13. Dumschat, C.; Borchardt, M.; Diekmann, C.; Cammann, K.; Knoll, M. *Sens. Actuators B* **1995**, *24-25*, 279-281.
14. Novell, M.; Parrilla, M.; Crespo, G. A.; Rius, F. X.; Andrade, F. J. *Anal. Chem.* **2012**, *84*, 4695-4702.